


Article

Characteristics of Potentially Toxic Elements, Risk Assessments, and Isotopic Compositions (Cu-Zn-Pb) in the PM₁₀ Fraction of Road Dust in Busan, South Korea

Hyeryeong Jeong ^{1,2} and Kongtae Ra ^{1,2,*} 

¹ Marine Environmental Research Center, Korea Institute of Ocean Science and Technology (KIOST), Busan 49111, Korea; hrjeong@kiost.ac.kr

² Department of Ocean Science (Oceanography), KIOST School, University of Science and Technology (UST), Daejeon 34113, Korea

* Correspondence: ktra@kiost.ac.kr

Abstract: The pollution status of ten potentially toxic elements (PTEs), isotopic compositions (Cu, Zn, Pb), and the potential ecological risk posed by them were investigated in the PM₁₀ fraction of road dust in Busan Metropolitan city, South Korea. Enrichment factors revealed extremely to strongly polluted levels of Sb, Cd, Zn, Pb, and Cu in the PM₁₀ fraction of road dust, with Sb levels being the highest. Statistical analyses showed that the major cause for contamination with PTEs was non-exhaust traffic emissions such as tire and brake wear. Cu and Zn isotopic compositions of road dust were related to traffic-related emission sources such as brake and tires. Pb isotopic compositions were close to that of road paint, indicating that Pb was a different source from Cu and Zn in this study. No significant health risk was posed by the PTEs. Taking into account the total length of road in Busan, a high quantity of PTEs in road dust (PM₁₀) can have serious deleterious effects on the atmospheric environment and ecosystems. The results of metal concentrations and isotopic compositions in road dust will help identify and manage atmospheric fine particle and coastal metal contamination derived from fine road dust.

Keywords: road dust; particulate matter; potentially toxic elements; Cu-Zn-Pb isotopes; risk assessment



Citation: Jeong, H.; Ra, K. Characteristics of Potentially Toxic Elements, Risk Assessments, and Isotopic Compositions (Cu-Zn-Pb) in the PM₁₀ Fraction of Road Dust in Busan, South Korea. *Atmosphere* **2021**, *12*, 1229. <https://doi.org/10.3390/atmos12091229>

Academic Editors: Salah Khardi and Nathalie Bernoud-Hubac

Received: 3 September 2021

Accepted: 17 September 2021

Published: 19 September 2021

Publisher's Note: MDPI stays neutral with regard to jurisdictional claims in published maps and institutional affiliations.



Copyright: © 2021 by the authors. Licensee MDPI, Basel, Switzerland. This article is an open access article distributed under the terms and conditions of the Creative Commons Attribution (CC BY) license (<https://creativecommons.org/licenses/by/4.0/>).

1. Introduction

The acceleration of urbanization and the growth of population in cities has increased the magnitude of the negative environmental impact caused by road dust [1]. The total length of roads in Korea in 2019 was 110,714 km, which is an increase of 5401 km over the previous five years [2]. Vehicles are the main contributors of various contaminants that constitute road dust. The number of vehicles in Korea increased from 20.1 million in 2014 to 23.7 million in 2019. Therefore, environmental pollution caused by road dust in urban environments has attracted considerable attention.

Potentially toxic elements (PTEs) are pollutants that can accumulate in the environment because of traffic as well as industrial and mining activities [3–5]. The presence of PTEs in road dust, soils, and atmospheric particulate matter have been reported in many countries [6–13]. The concentrations of PTEs in road dust are used as indicators of environmental pollution and for the identification of pollution sources such as traffic and industrial activities.

The fine particles in road dust have a much higher concentration of PTEs compared to coarse particles [14–16]. The fine particles (<10 μm) in road dust are easily resuspended into the atmosphere by wind and vehicle movement, and thus, they can be transported over a long distance [16–18]. PTEs in fine road dust can pose a greater health risk to the human body via ingestion, inhalation, and dermal contact pathways [19–26].

Fine road dust is an important source of PTE contamination in urban atmosphere and soils. Fugitive road dust particles caused by vehicle movement on paved roads are emitted from the road to the surrounding atmosphere because of turbulence and contribute significantly to the concentration of PM₁₀ in the atmospheric environment [27–29]. The contribution of fugitive dust to total particulate matter is gaining importance because of the increase in the number of vehicles and the detrimental health impacts of high concentrations of heavy metals contained in them [30–32]. Several studies have reported that fugitive road dust accounts for 14% to 55% of PM₁₀ concentrations in India [33], Brazil [34], and European urban areas [35]. In Korea, PM₁₀ contributes more than 60% of the fine dust that is re-suspended from the paved road [36].

Souto-Oliveira et al. [37] studied the source contribution in aerosol using Cu, Zn, and Pb multi-isotopes. According to atmospheric emission inventory of the PM₁₀ sources, road transport and resuspension contributed 40% and 25% in Sao Paulo and 48% and 21% in London, respectively. Cu-Zn [38–40], Zn [41,42], and Pb [43–45] isotopes are used for identifying anthropogenic/natural sources in various environmental samples. Recently, multi-isotope studies using Cu, Zn, and Pb have been conducted to determine pollution sources in atmospheric environments [37,46,47].

The purpose of this study is to (1) characterize the PTEs in fine particulate matter (PM₁₀) of road dust in Busan Metropolitan in South Korea; (2) assesses the potential ecological risk and non-carcinogenic health risk posed by them; (3) present Cu, Zn, and Pb isotope compositions as a preliminary study for identifying potential pollution sources.

2. Materials and Methods

2.1. Study Area

The Busan Metropolitan City is the largest port city in South Korea. Busan is located in the southeastern part of South Korea and has a land area of 506 km² and an impermeable area of 234.31 km². Busan has a population of 3.4 million, and the population density of the impermeable area is 14,570 persons/km². The average temperature, precipitation, humidity, and wind speed over the past 30 years are 14.7 °C, 1519 mm, 64.7%, and 13.3 km/h, respectively. The road dust in Busan is contaminated with Sb, Cu, Cd, Zn, and Pb caused by transportation activities, and these toxic elements present on the road surfaces are transported to coastal areas through runoff during precipitation [48].

2.2. Sampling and Measurement of PTEs

Road dust samples were collected from 25 sites in Busan during May 2014. The sampling locations and the study area are shown in Figure 1. Road dust was obtained using a cordless vacuum cleaner (DC35, Dyson Limited, Malmesbury, UK) covering an area of 0.25 m² (0.5 m × 0.5 m) from the curb, and each composite sample comprised of 4–5 subsamples to ensure representativeness. The vacuum cleaner was disassembled and cleaned prior to sampling at each site to prevent cross contamination. The samples were stored in a zipper bag, dried in an oven at 40 °C, and weighed. Road dust containing particles of less than 10 µm (PM₁₀) size was separated using a nylon sieve and a vibratory sieve shaker (Analysette 3 PRO, Fritsch GmbH, Germany) in the laboratory.

The analysis of PTEs in the PM₁₀ fraction of road dust was performed through total digestion using a high-purity (Suprapur[®] grade) acid mixture containing HNO₃, HF, and HClO₄. About 0.1 g of the sample was decomposed in a Teflon digestion vessel using the acid mixture on a hot plate at 180 °C, evaporated, and then redissolved using 2% HNO₃. Al, Cr, Co, Ni, Cu, Zn, As, Cd, Sb, and Pb were measured using inductively coupled plasma mass spectrometry (ICP-MS, iCAP-Q, Thermo Fisher Scientific, Braunschweig, Germany). Hg was measured using a Hg analyzer (Hydra-C, Teledyne Leeman Labs, Hudson, NH, USA). Duplicate measurements were performed to ensure the reliability of the analysis. Data accuracy was ensured using certified reference materials MESS-4 and PACS-3, and the recoveries ranged from 95.7% to 102.4%.

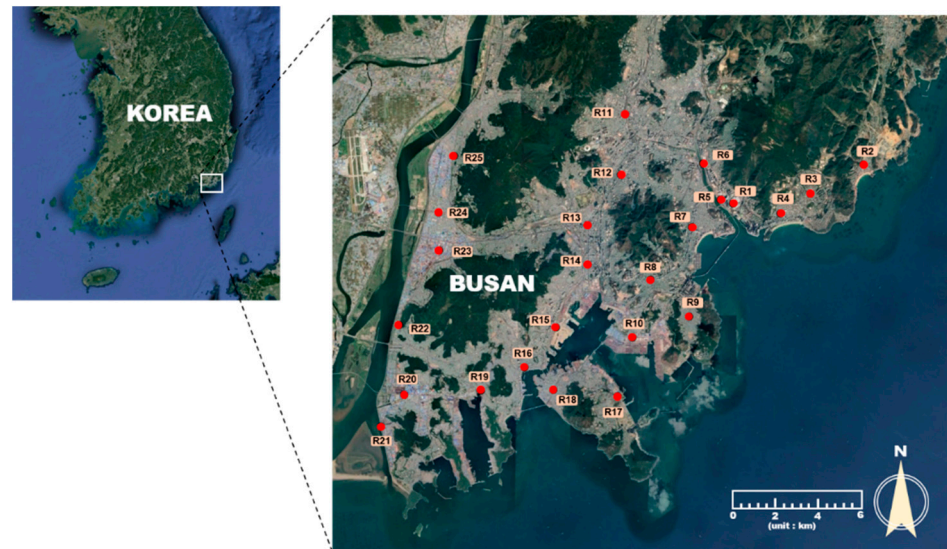


Figure 1. Sampling sites for road dust (RD) from the Busan metropolitan city, South Korea (base map from Google Earth).

2.3. Pollution and Ecological Risk Assessments

The enrichment factor (EF) was used to assess the contamination levels of individual metals using the following equation [49]:

$$EF = \frac{(PTEs/Al)_{samples}}{(PTEs/Al)_{background}}. \quad (1)$$

The EF values were classified into five classes [50], and the classification is provided in Table S1.

Single factor ecological risk degree (E_r^i) and potential ecological risk (PER) were used to assess the ecological risk of the ten PTEs on their toxicity response using the following equations [51]:

$$E_r^i = T_r^i \times (C_i/B_i); \quad PER = \sum_i^n E_r^i \quad (2)$$

where C_i and B_i are the measured and geological background concentrations by Rudnick and Gao [52], respectively, T_r^i is the toxic response factor (Hg = 40, Cd = 30, As = 10, Sb = 7, Co = Cu = Ni = Pb = 5, Cr = 2, and Zn = 1) [51,53,54]. E_r^i and PER values were classified into five and four classes, respectively (Table S1).

2.4. Health Risk Assessment

Health risk assessment was carried out considering the exposure of adults and children, through the pathways of ingestion, inhalation, and dermal contact, to the ten PTEs present in the PM_{10} fraction of road dust by calculating the non-carcinogenic hazards based on the guidelines of [55,56].

The average daily dose (ADD) for the exposure assessment of PTEs via ingestion (ADD_{ing}), inhalation (ADD_{inh}), and dermal contact (ADD_{derm}) were calculated using the follow equations:

$$ADD_{ing} = C_i \times \left(\frac{IngR \times EF \times ED}{BW \times AT} \right) \times 10^{-6} \quad (3)$$

$$ADD_{inh} = C_i \times \left(\frac{IngR \times EF \times ED}{PEF \times BW \times AT} \right) \quad (4)$$

$$ADD_{derm} = C_i \times \left(\frac{SL \times SA \times ABS \times EF \times ED}{BW \times AT} \right) \times 10^{-6} \quad (5)$$

where C_i represents the concentration of PTEs (mg/kg) in the PM_{10} fraction of road dust. All the other parameters present in these equations and their corresponding values for adults and children are provided in Table S2 [57].

The hazard quotient (HQ) was calculated using the rate of the corresponding reference dose (RfD) for each exposure pathway i to determine the non-carcinogenic risks posed by the PTEs in road dust. The RfD values reported by Ferreira-Baptista and De Miguel [58] and Ma et al., [59] were used in this study.

$$HQ_i = \frac{ADD_i}{RfD_i} \quad (6)$$

If $HQ > 1$, a potential adverse health effect may occur, whereas if $HQ < 1$, an adverse health effect will not occur.

The hazard index (HI) for each PTE was also calculated using the following equation:

$$HI = HQ_{ing} + HQ_{inh} + HQ_{derm} \quad (7)$$

If the HI value exceeds the threshold value of 1, non-carcinogenic effects are likely to occur.

2.5. Measurement of Cu, Zn, and Pb Isotopes

Isotopic compositions of Cu, Zn, and Pb isotopes were measured using multi-collector ICP-MS (MC-ICP-MS) at the Korea Institute of Ocean Science and Technology (KIOST). Analytical methods and instrumental settings followed [48]. The Cu and Zn isotopic data for each sample represent the average of 3–4 standard sample brackets. Samples of 100–200 ppb were introduced into the Teflon nebulizer through a $100 \mu\text{L min}^{-1}$. Cu and Zn isotopic compositions are expressed in delta notation from isotopic standards (ERM-AE647, IRMM-3702).

$$\delta^{65}\text{Cu} = \left(\frac{(^{65}\text{Cu}/^{63}\text{Cu})_{\text{sample}}}{(^{65}\text{Cu}/^{63}\text{Cu})_{\text{ERM-AE647}}} - 1 \right) \times 1000 \quad (8)$$

$$\delta^{66}\text{Zn} = \left(\frac{(^{66}\text{Zn}/^{64}\text{Zn})_{\text{sample}}}{(^{66}\text{Zn}/^{64}\text{Zn})_{\text{IRMM-3702}}} - 1 \right) \times 1000 \quad (9)$$

3. Results and Discussion

3.1. Characteristics of PTEs in Road Dust (<10 μm)

3.1.1. Concentrations of PTEs

The concentrations of PTEs in the PM_{10} fraction of road dust are summarized in Table 1. The spatial distribution of these elements is illustrated in Figure S1. The average concentrations of PTEs in the PM_{10} fraction of the road dust are as follows: Zn (3007 mg/kg), Cu (513 mg/kg), Pb (480 mg/kg), Cr (300 mg/kg), Ni (75.6 mg/kg), Sb (61.6 mg/kg), Co (19.8 mg/kg), As (17.0 mg/kg), Cd (5.6 mg/kg), and Hg (0.6 mg/kg) (Figure 2a).

High concentrations of Cu, Zn, Cd, Pb, and Hg were observed in sampling sites R11–R16 that experience heavy traffic because of the presence of large departmental stores, city halls, and fish markets. Many studies have reported that pollution by these elements is mainly caused by traffic activities [60–63]. Previous studies have reported that heavy traffic intensity contributes to high levels of heavy metals in the fine size fraction of road dust [64–67]. In this study, the concentrations of PTEs were relatively low in sampling sites that experience low traffic volume and areas with smaller road widths.

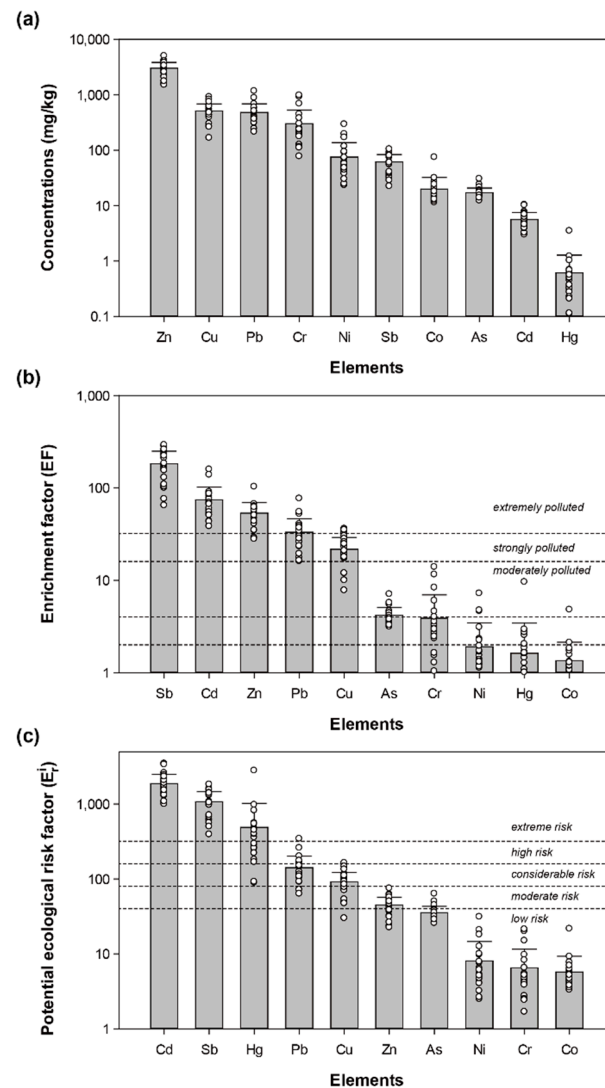


Figure 2. Comparison of mean ± standard deviation (1 s) values for concentrations (a), enrichment factor (b), and potential ecological risk factor (c) of PTEs in PM₁₀ of road dust in this study.

Table 1. Comparison of mean values for PTEs concentrations (mg/kg) in PM₁₀ of road dust and those in the other published data.

Cr	Co	Ni	Cu	Zn	As	Cd	Sb	Pb	Hg	Sample Size
300	19.8	75.6	513	3007	17.0	5.6	61.6	480	0.6	<10 µm (this study)
182	-	109	287	1829	-	0.9	-	456	-	<20 µm ¹
373	-	296	333	819	-	2	29	233	-	2.5~10 µm ²
196	26	121	550	2038	-	3.7	85	234	-	<20 µm ³
75.5			113	591		0.6		112		<44 µm ⁴
176	8.87	48.3	376	1150				406		<50 µm ⁵
576	28.9			2945			33.5			1.8~10 µm ⁶
			822	1000	5.4	3.4	11	313		<37 µm ⁷
53.8	9.3	34.2	100	302	17.0	0.6		48.8		<10 µm ⁸
	34		270	470		1.9		148		<2 µm ⁹
68	15	46	184	1026		0.8	12	91		<10 µm ¹⁰

¹ Adamiec et al., 2016 [61] (road-deposited sediment); ² Padoan et al., 2017 [66] (road dust); ³ Adamiec and Jarosz-Krzemińska 2019 [57] (sidewalk dust); ⁴ Zhao et al., 2010 [67] (road-deposited sediments); ⁵ Bi et al., 2013 [68] (road dust); ⁶ Levesque et al., 2021 [69] (urban dust); ⁷ Fujiwara et al., 2011 [70] (road dust); ⁸ Kong et al., 2012 [14] (road dust); ⁹ Logiewa et al., 2020 [16] (road dust at Krakow); ¹⁰ Vlasov et al., 2021 [21] (road dust).

The highest concentrations of Cr, Ni, and Co were observed in sampling sites R21 and R23 that are located in an industrial area containing metal- and steel-related facilities (processing and cutting). Cr and Ni are the most common metals used for alloying because of their high hardness and corrosion resistance, and they are widely used in steel production. Daigo et al. [71] reported that 85% and 61% of the global production of Cr and Ni, respectively, are used in stainless steel production. Stainless steel contains more than 10% of Cr and Ni. Various alloying metals are extensively used in food, beverage, and medical industries and in the manufacturing of equipment, machinery, and vehicle. Co is released from stainless steel and Ni-based alloy powders and Cr-alloy powders [72,73]. The highest concentrations of Sb and Pb were found in R22, which has a tire replacement shop. Particles released from the tire and brake pad replacement process spread to the surrounding, resulting in a high concentration of these elements in road dust.

The average concentrations of Co, Ni, Cu, Zn, Cd, Sb, Pb, and Hg in the PM₁₀ fraction of road dust were 1.1 (Ni)–4.1 (Hg) times higher than those of the bulk road dust samples [48]. The concentrations of PTEs in this study were lower than that of the soil pollution standard for roads and factory sites in Korea [74]; however, they were higher than the fine particulate fraction of road dust in other cities [14,16,21,57,61,67,69,70,75].

3.1.2. Pollution Assessment of PTEs

The average EF value of Sb was the highest among the PTEs (average 183 mg/kg, minimum: 64.8 mg/kg, and maximum: 292 mg/kg). The average of EF values occurs in the following order: Sb > Cd > Zn > Pb > Cu > As > Cr > Ni > Hg > Co (Figure 2b). The Sb and Cd in the PM₁₀ fraction of the road dust had EF values exceeding 32, indicating the extremely polluted level at all the sampling sites. The average EF value for Zn (53.4) indicates an extremely polluted level. The average EF of Cu was 21.7, which corresponds to the strongly polluted level with three sampling sites corresponding to the extremely polluted level. The reasons for the high levels of contamination with Sb, Cu, Zn, and Cd are wearing of brakes and tires [70,76,77].

Substantial quantities of Sb compounds are used in the production of polyethylene terephthalate as catalysts and brake pads as lubricants [78,79]. Of the 54 µg of Sb emitted per braking event per car, 32 µg is apportioned in the PM₁₀ fraction and 22 µg is apportioned in the PM_{2.5} fraction [76,80,81]. Bukowiecki et al. [82] reported that the Sb emission factors of Sb were 11 µg km⁻¹ vehicle⁻¹ for light-duty vehicles and 86 µg km⁻¹ vehicle⁻¹ for heavy-duty vehicles. Garg et al. [83] concluded that about 30% of brake wear was released into the airborne particulate matter and the emission rate ranged from 3.3 to 8.8 mg/km. Extreme enrichment of Sb in road dust, stream sediments, and particulate matter in runoff has been observed in Korea [48,84,85]. The average values of EF for As show that the PM₁₀ fraction of road dust was moderately polluted, and Cr, Ni, Hg, and Co were slightly polluted to unpolluted levels.

3.1.3. Ecological Risk Assessments

A comparison of the single factor ecological risk degree (E_r^i) for the measured PTEs is presented in Figure 2c. The average E_r^i values of Cd (1872), Sb (1078), and Hg (489) exceeded 320, which indicates that these elements in the PM₁₀ fraction of road dust correspond to the extreme ecological risk level because of their high concentrations. The average E_r^i values of the PTEs in the descending order were as follows: Cd > Sb > Hg > Pb > Cu > Zn > As > Ni > Cr > Co. The average E_r^i values of Pb and Cu indicate considerable potential risk.

The average E_r^i value of Zn was 44.9, indicating moderate potential risk. The average E_r^i value of As, Ni, Cr, and Co were less than 40, indicating low potential risk. The average PER value (3772), which represents the comprehensive ecological risk of the ten PTEs, significantly exceeded 600, indicating high ecological risk for all the sampling sites in the PM₁₀ fraction of road dust.

3.1.4. Health Risk Assessments

The values of the HQ and HI are provided in Table 2. For adults, the average values of HQ_{ing} , HQ_{inh} , and HQ_{derm} were <1, indicating no non-carcinogenic risks posed by PTEs in the PM_{10} fraction of road dust (Figure 3). The HQ_{ing} values of Cr, Cd, and Sb were higher than those of HQ_{inh} and HQ_{derm} . The average HI values for adults in decreasing order were as follows: $Sb > Cr > Pb > As > Cd > Cu > Zn > Ni > Co > Hg$ (Figure 3a). The HI for adults was <1, indicating no non-carcinogenic health risk by PTEs in the PM_{10} fraction of road dust.

Table 2. The results of hazard quotient (HQ) and hazard index (HI) of non-carcinogenic hazards for potentially toxic elements in PM_{10} of road dust.

Metals	Adult				Children			
	HQ_{ing}	HQ_{inh}	HQ_{derm}	HI	HQ_{ing}	HQ_{inh}	HQ_{derm}	HI
Cr	3.5×10^{-2}	2.8×10^{-3}	4.0×10^{-2}	7.8×10^{-2}	3.3×10^{-1}	2.6×10^{-2}	9.2×10^{-2}	4.5×10^{-1}
Ni	1.3×10^{-3}	1.0×10^{-6}	1.1×10^{-4}	1.4×10^{-3}	1.2×10^{-2}	9.4×10^{-6}	2.6×10^{-4}	1.3×10^{-2}
Co	3.5×10^{-4}	9.3×10^{-4}	9.9×10^{-6}	1.3×10^{-3}	3.3×10^{-3}	8.7×10^{-3}	2.3×10^{-5}	1.2×10^{-2}
Cu	4.5×10^{-3}	3.4×10^{-6}	3.4×10^{-4}	4.9×10^{-3}	4.2×10^{-2}	3.2×10^{-5}	7.9×10^{-4}	4.3×10^{-2}
Zn	3.5×10^{-3}	2.7×10^{-6}	4.0×10^{-4}	3.9×10^{-3}	3.3×10^{-2}	2.5×10^{-5}	9.2×10^{-4}	3.4×10^{-2}
As	2.0×10^{-2}	1.5×10^{-5}	1.1×10^{-3}	2.1×10^{-2}	1.9×10^{-1}	1.4×10^{-4}	2.5×10^{-3}	1.9×10^{-1}
Cd	2.0×10^{-3}	1.5×10^{-6}	4.5×10^{-3}	6.5×10^{-3}	1.8×10^{-1}	1.4×10^{-5}	1.0×10^{-2}	2.9×10^{-2}
Sb	5.4×10^{-2}	4.1×10^{-5}	6.2×10^{-2}	1.2×10^{-1}	5.1×10^{-1}	3.8×10^{-4}	1.4×10^{-1}	6.5×10^{-1}
Pb	4.8×10^{-2}	3.7×10^{-5}	7.3×10^{-3}	5.6×10^{-2}	4.5×10^{-1}	3.4×10^{-4}	1.7×10^{-2}	4.7×10^{-1}
Hg	7.2×10^{-4}	5.5×10^{-7}	2.3×10^{-4}	9.5×10^{-4}	6.7×10^{-3}	5.1×10^{-6}	5.4×10^{-4}	7.2×10^{-3}
Sum	1.7×10^{-1}	3.8×10^{-3}	1.2×10^{-1}	2.9×10^{-1}	1.6	3.6×10^{-2}	2.7×10^{-1}	1.9

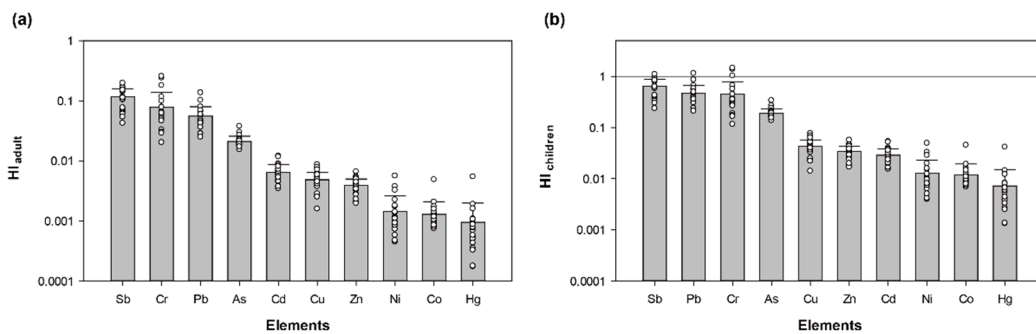


Figure 3. Comparison of mean \pm standard deviation (1 s) values for hazard index (HI) for adult (a) and children in PM_{10} of road dust in this study (b).

The average value of HQ for children in terms of non-carcinogenic risk through the three pathways was less than 1. The HI values for children were higher than those for adults. However, HQ_{ing} values of the sampling sites in industrial areas for Cr and Pb were >1, indicating that potential adverse health effects can occur. HQ_{inh} and HQ_{derm} values of all the sampling sites and PTEs were <1. The HI values for children were in the decreasing order as follows: $Sb > Pb > Cr > As > Cu > Zn > Cd > Ni > Co > Hg$ (Figure 3b). The HI values for children in industrial areas (R21, R23, and R25) for Cr and near the tire replacement facility (R22) for Sb and Pb exceeded 1, indicating a potential non-carcinogenic effect of the PM_{10} fraction of road dust. The total HQ values of PTEs for both adults and children decreased in the following order: ingestion > dermal contact > inhalation in the PM_{10} fraction of road dust (Table 2). This suggests that ingestion is the major exposure pathway for most toxic elements except for Cr, Cd, and Sb for adults and children. Dermal contact was the main exposure pathway for Cr, Cd, and Sb. The HI value for children was higher than that for adults.

The quantity of the PM_{10} fraction in road dust per unit area of road surface ranged from 0.01 to 6.9 g/m^2 with an average of 2.4 g/m^2 . The average quantities of PTEs in

the PM₁₀ fraction of road dust were 0.71 mg/m² for Cr, 0.05 mg/m² for Co, 0.19 mg/m² for Ni, 1.26 mg/m² for Cu, 7.75 mg/m² for Zn, 0.04 mg/m² for As, 0.01 mg/m² for Cd, 0.15 mg/m² for Sb, 1.29 mg/m² for Pb, and 0.001 mg/m² for Hg, respectively. Considering the total length of paved roads in Busan at 3313 km, significant quantities of PTEs have accumulated on the road surfaces in its urban area.

3.2. Pollution Source and Environmental Impact of PTEs in the PM₁₀ Fraction of Road Dust

3.2.1. Statistical Analysis

To understand the sources of the PTEs, principal component analysis (PCA) and Pearson's correlation analysis were conducted using SPSS (version 18.0). The Kaiser–Meyer–Olkin (KMO) test value was 0.625, and the Bartlett test result was $p < 0.001$, indicating that the data set was suitable for PCA analysis. Two principal components explaining 63.0% of the total variance were extracted (Figure 4). PC1 explained 40.8% of the total variance, and it had a positive loading on Cu, Zn, Cd, Sb, and Pb with a strong positive correlation between these elements (Table 3). The PCA result and the significant degree of pollution of these elements in road dust are attributed to traffic sources. PC2 explained 22.2% of the total variance, and it had a positive loading on Cr, Co, and Ni with positive correlations between them. The pollution levels of these elements were not significant, and these are attributed to natural origins except for sampling sites in industrial areas.

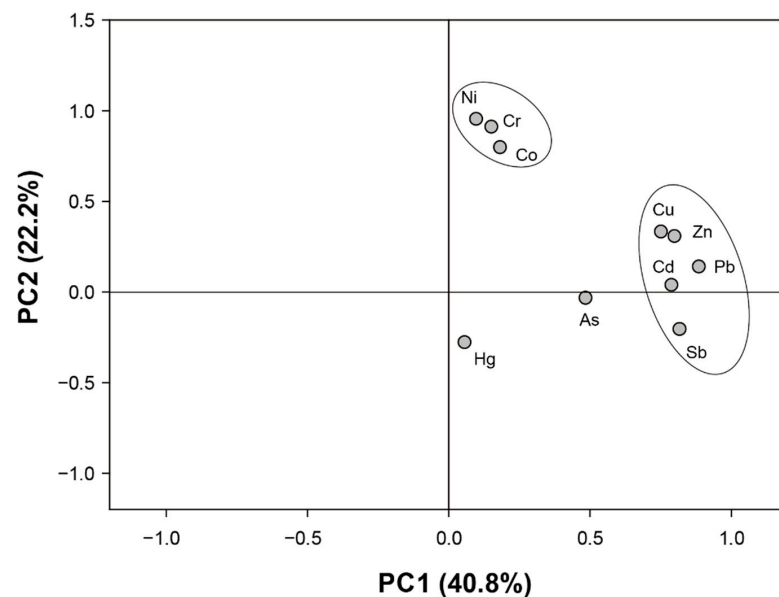


Figure 4. Component-loading plot for the principal component analysis of the potentially toxic elements in this study.

Table 3. Pearson's correlation of the potentially toxic elements in PM₁₀ of road dust. Bold indicates that correlation significant at 0.01 level.

	Cr	Co	Ni	Cu	Zn	As	Cd	Sb	Pb	Hg
Cr	-									
Co	0.615	-								
Ni	0.925	0.672	-							
Cu	0.415	0.304	0.348	-						
Zn	0.315	0.370	0.371	0.703	-					
As	0.031	0.129	0.060	0.139	0.107	-				
Cd	0.094	0.210	0.082	0.511	0.798	0.143	-			
Sb	0.02	-0.023	-0.108	0.589	0.457	0.411	0.498	-		
Pb	0.243	0.275	0.244	0.616	0.679	0.642	0.582	0.644	-	
Hg	-0.127	-0.189	-0.170	-0.010	0.058	-0.215	0.022	0.104	-0.449	-

3.2.2. Elemental Ratios

Some researchers have found that brake and tire wear show a specific pattern of some heavy metals such as Fe, Ti, Cu, Zn, Zr, Mo, Sn, Sb, Cd, and Pb [86–89]. In many studies, elemental concentrations and ratios between elements such as Zn/Cu and Cu/Sb were used as tracers to evaluate the relative contributions and contamination sources of PTEs in road dust [90–92]. Since brake pads and linings contain Sb_2O_3 and Sb_2S_3 , a high concentration of Sb is present in road dust and atmospheric particulate matter [93]. The EF values show that Sb contamination was more than that of other elements. PM_{10} emission factors from brake and tire wear were reported at 2.9–7.5 mg and 3.0–13.0 mg km^{-1} vehicle⁻¹, respectively [83,94–98]. The total number of vehicles in Busan is 1.4 million, and the average daily driving distance is 39.6 km vehicle⁻¹. Therefore, a substantial quantity of PTEs generated by these traffic activities would have accumulated on the road surface.

Sanders et al. [99] reported that 50–70% of the total wear lining material was released in the form of airborne particles. Grigoratos and Martini [100] reported that brake wear can contribute up to 55% of the mass of the total non-exhaust traffic-related PM_{10} emissions and up to 21% of the mass of the total transportation-related PM_{10} emissions in urban environments. Tires lose approximately 1.0–1.5 kg of weight over their lifetime, of which the PM_{10} percentage is less than 10% [101,102]. In this study, the average Zn/Cu and Cu/Sb ratios were 6.1 ± 1.3 and 8.9 ± 3.4 , respectively. This indicates that the dominant pollution source of the PM_{10} fraction of the road dust was non-exhaust traffic activities such as wear of brakes and tires.

3.2.3. Cu, Zn, and Pb Isotopic Compositions

Cu isotopic compositions ($\delta^{65}\text{Cu}_{\text{AE647}}$) of road dust (<10 μm) in this study ranged from -0.04 to $+0.13\text{‰}$ (mean: $+0.05\text{‰} \pm 0.05$, sd, $n = 25$). The $\delta^{65}\text{Cu}_{\text{AE647}}$ values of road dust (<10 μm) were closer to those of the brake pads from Korea (unpublished data) than brake pads from the UK [103] (Figure 5a). It also indicates that the isotopic compositions of the brake pads can differ depending on the manufacturers. Zn isotopic compositions ($\delta^{66}\text{Zn}_{\text{IRMM3702}}$) of road dust (<10 μm) in this study ranged from -0.17 to -0.03 (mean: $-0.11\text{‰} \pm 0.03$, sd, $n = 25$). Road dust (<10 μm) was distinguished from road paint (UK; [103]) and brake pads (UK; [103]) in the plot of concentrations and isotopic compositions of Zn. However, road dust (<10 μm) was similar to brake pads (Korea; unpublished data) and tires (UK; [103]) in Figure 5b, suggesting that the Zn sources in road dust were closely related to traffic-related sources. Previous studies reported that brake pads and tires had significantly high Cu and Zn concentrations, respectively, and these were major sources of road dust from traffic-related emissions [88,95]. Our results also showed that Cu and Zn sources of road dust (<10 μm) were associated with traffic-related emissions. The Pb isotopic composition ($^{206}\text{Pb}/^{207}\text{Pb}$) of road dust (<10 μm) in this study ranged from 1.1432 to 1.1606 (mean: 1.1514 ± 0.0036 , sd, $n = 25$). Road dust (<10 μm) overlapped with road paint (UK; [103]) and was distinguished from brake pads (UK; [103], Korea; unpublished data) and tires (UK) in Figure 5c. Previous study reported that the mean of $^{206}\text{Pb}/^{207}\text{Pb}$ values in lead-based paint ranged from 1.083 to 1.183 (mean: 1.117 ± 0.030 , sd, $n = 15$; [104]). Anthropogenic Pb sources in urban environments derive from various sources such as lead-based paint, traffic-related exhaust, and industrial activities [105]. Additionally, lead-based paints are common sources of lead-contaminated soil and road dust [106–108]. Pb sources of road dust (<10 μm) in this study appear to be different sources from Zn and Cu.

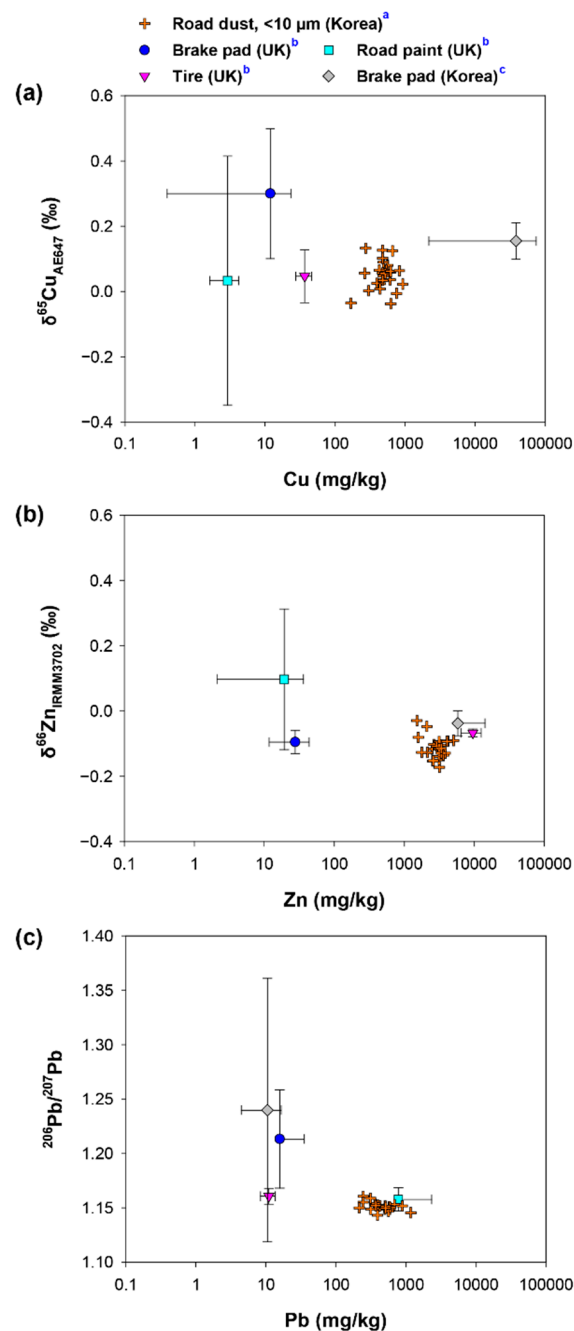


Figure 5. Plots of concentrations versus isotopic compositions of Cu, Zn, and Pb ((a): this study, (b): Dong et al., 2017 [103], (c): unpublished data).

The average $\delta^{65}\text{Cu}_{\text{AE647}}$ and $\delta^{66}\text{Zn}_{\text{IRMM3702}}$ values of this study are slightly higher than those of heavily industrialized areas [109]. On the other hand, the average $^{206}\text{Pb}/^{207}\text{Pb}$ ratio of this study had a lower value than industrial areas [109]. In the plots of concentration and isotopic composition for Cu and Pb, the urban area (this study) can be clearly distinguished from the industrial area (Figure S2) [109]. This industrial area provided a clear signal, as it was heavily contaminated with Cu and Pb compared to Zn. Additionally, it was difficult to distinguish between urban and industrial areas in the plot of concentration and isotopic values for Zn (Figure S2).

Recent studies reported the contribution of pollution sources using various modeling programs (Iso-source, SIAR, PMF) in atmospheric fine dust [110–112]. Endmembers of various pollution sources will enable more accurate source tracking, and evaluation of the contribution rate for specific pollutants using these models can help improve source

identification. However, metallic isotope fingerprints of various pollution sources are still insufficient in South Korea. Therefore, it is important to collect endmembers of various pollutants to trace these sources precisely by applying these models in further study. Especially, isotopic fingerprints of products from each country are also needed, since traffic-related sources may differ depending on the manufacturing countries.

4. Conclusions

Recently, PTEs in the fine particle fraction of road dust have been attracting significant attention because they can easily resuspend and affect the atmosphere and human health. Ten PTEs in the PM₁₀ fraction of road dust from the port city of Busan were investigated to evaluate the pollution status, identify isotopic compositions (Cu, Zn, Pb), and assess the potential ecological risks posed by them. The average concentrations of the studied PTEs (mg/kg) in decreasing order are as follows: Zn (3007) > Cu (513) > Pb (480) > Cr (300) > Ni (75.6) > Sb (61.6) > Co (19.8) > As (17.0) > Cd (5.6) > Hg (0.6). The enrichment factors showed extremely polluted level in terms of Sb, Cd, Zn, and Pb, and strongly polluted levels for Cu. Based on average EF value, the PTEs can be ranked as follows: Sb > Cd > Zn > Pb > Cu > As > Cr > Ni > Hg > Co. Ecological risk assessment indicated that the PM₁₀ fraction of road dust poses extreme risk of Cd, Sb, and Hg contamination, considerable risk of Pb and Cu, and moderate risk of Cu. Considering the high total length of road in the study area and the quantity of PM₁₀ contained in the road dust, some PTEs (Sb, Cd, Zn, Pb, and Cu) can seriously affect the atmospheric environment and human health. The degree of pollution and statistical analyses such as Pearson's correlation and PCA analysis showed that the PTEs in the PM₁₀ fraction of road dust were mainly due to the abrasion of tires and brake pads. The result of Cu isotopic compositions ($\delta^{65}\text{Cu}_{\text{AE647}}$) indicated that Cu source of road dust (<10 μm) was more related to brake pads from Korea than that of the UK. The $\delta^{66}\text{Zn}_{\text{IRMM3702}}$ had similar values to brake pads (Korea) and tires (UK), indicating Zn source associated with traffic-related emission sources. Pb isotopic ratios ($^{206}\text{Pb}/^{207}\text{Pb}$) of road dust (<10 μm) were close to road paint (UK), suggesting that the dominant Pb source in this study was different from Cu and Zn. The approach using multi-isotope has been successfully carried out, and it is meaningful to compare the isotopic composition of road dust (<10 μm) with potential pollution sources in this study. Long-term monitoring is required to efficiently reduce/manage fine road dust polluted with high concentrations of PTEs and to understand the impact of PTEs in road dust on the environments and the relationship between road dust and atmospheric particles.

Supplementary Materials: The following are available online at <https://www.mdpi.com/article/10.3390/atmos12091229/s1>, Figure S1: Spatial distribution of potentially toxic elements in PM₁₀ of road dust in this study, Figure S2: Plots of concentrations and isotopic values of Cu, Zn, and Pb (a: this study, b: Jeong et al., 2021), Table S1: Classification of enrichment factor (EF) and potential ecological risk factor (E_r^I) for each element and potential ecological risk index (PER), Table S2: Key parameters for the health risk assessment through three pathways used in this study (USEPA, 2011;2016, Zhou et al., 2015; Adamiec, 2017).

Author Contributions: Conceptualization, data curation, writing—original draft preparation, writing—review and editing, H.J. and K.R.; formal analysis, investigation, validation, H.J.; methodology, funding acquisition, project administration, resources, supervision, visualization, K.R. All authors have read and agreed to the published version of the manuscript.

Funding: This research was funded by Korea Institute of Ocean Science and Technology (KIOST), grant number PE99912.

Institutional Review Board Statement: Not applicable.

Informed Consent Statement: Not applicable.

Data Availability Statement: All data for this study are available from the corresponding author on request.

Acknowledgments: We thank the anonymous reviewers for their valuable comments to improve our study.

Conflicts of Interest: The authors declare no conflict of interest.

References

1. Trujillo-Gonzalez, J.M.; Torres-Mora, M.A.; Keesstra, S.; Brevik, E.C.; Jimenez-Ballesta, R. Heavy metal accumulation related to population density in road dust samples taken from urban sites under different land uses. *Sci. Total Environ.* **2016**, *553*, 636–642. [[CrossRef](#)] [[PubMed](#)]
2. KOSIS (Korean Statistical Information Service). 2021. Available online: www.kosis.kr (accessed on 19 September 2021).
3. Khan, A.; Khan, S.; Khan, M.; Qamar, Z.; Waqas, M. The uptake and bioaccumulation of heavy metals by food plants, their effects on plants nutrients, and associated health risk: A review. *Environ. Sci. Pollut.* **2015**, *22*, 13772–13799. [[CrossRef](#)]
4. Lv, J.; Wand, Y. PMF receptor models and sequential Gaussian simulation to determine the quantitative sources and hazardous areas of potentially toxic elements in soils. *Geoderma* **2019**, *353*, 347–358. [[CrossRef](#)]
5. Liu, P.; Zhang, Y.; Feng, N.; Zhu, M.; Tian, J. Potentially toxic element (PTE) levels in maize, soil, and irrigation water and health risks through maize consumption in northern Ningxia, China. *BMC Public Health* **2020**, *20*, 1729. [[CrossRef](#)]
6. Capra, G.F.; Coppola, E.; Odierna, P.; Grilli, E.; Vacca, S.; Buondonno, A. Occurrence and distribution of key potentially toxic elements (PTEs) in agricultural soils: A paradigmatic case study in an area affected by illegal landfills. *J. Geochem. Explor.* **2014**, *145*, 169–180. [[CrossRef](#)]
7. de Souza, E.S.; Fernandes, A.R.; de Souza Braz, A.M.; Sabino, L.L.L.; Alleoni, L.R.F. Potentially toxic elements (PTEs) in soils from the surroundings of the Trans-Amazonian Highway, Brazil. *Environ. Monit. Assess.* **2015**, *187*, 4074. [[CrossRef](#)]
8. Ali, M.U.; Liu, G.; Yousaf, B.; Abbas, Q.; Ullah, H.; Munir, M.A.M.; Fu, B. Pollution characteristics and human health risks of potentially (eco)toxic elements (PTEs) in road dust from metropolitan area of Hefei, China. *Chemosphere* **2017**, *181*, 111–121. [[CrossRef](#)] [[PubMed](#)]
9. Keshavarzi, B.; Najmeddin, A.; Moore, F.; Afshari, M.P. Risk-based assessment of soil pollution by potentially toxic elements in the industrialized urban and peri-urban areas of Ahvaz metropolis, southwest of Iran. *Ecotoxicol. Environ. Saf.* **2019**, *167*, 365–375. [[CrossRef](#)] [[PubMed](#)]
10. Roy, S.; Gupta, S.K.; Prakash, J.; Habib, G.; Baudh, K.; Nasr, M. Ecological and human health risk assessment of heavy metal contamination in road dust in the National Capital Territory (NCT) of Delhi, India. *Environ. Sci. Pollut. Res. Int.* **2019**, *26*, 30413–30425. [[CrossRef](#)]
11. Gruszecka-Kosowska, A.; Baran, A.; Wdowin, M.; Mazur-Kajta, K.; Czech, T. The contents of the potentially harmful elements in the arable soils of southern Poland, with the assessment of ecological and health risks: A case study. *Environ. Geochem. Health* **2020**, *42*, 419–422. [[CrossRef](#)]
12. Jeong, H.; Choi, J.Y.; Lim, J.S.; Ra, K. Pollution caused by potentially toxic elements present in road dust from industrial areas in Korea. *Atmosphere* **2020**, *11*, 1336. [[CrossRef](#)]
13. Jeong, H.; Choi, J.Y.; Ra, K. Potentially toxic elements pollution in road deposited sediments around the active smelting industry of Korea. *Sci. Rep.* **2021**, *11*, 7238. [[CrossRef](#)] [[PubMed](#)]
14. Kong, S.F.; Lu, B.; Ji, Y.Q.; Zhao, X.Y.; Bai, Z.P.; Xu, Y.H.; Liu, Y.; Jiang, H. Risk assessment of heavy metals in road and soil dusts within PM_{2.5}, PM₁₀ and PM₁₀₀ fractions in Dongying city, Shandong Province, China. *J. Environ. Monit.* **2012**, *14*, 791–803. [[CrossRef](#)] [[PubMed](#)]
15. Jeong, H.; Choi, J.Y.; Lee, J.; Lim, J.; Ra, K. Heavy metal pollution by road-deposited sediments and its contribution to total suspended solids in rainfall runoff from intensive industrial areas. *Environ. Pollut.* **2020**, *265*, 115028.
16. Logiewa, A.; Mizagowicz, A.; Krennhuber, K.; Lanzerstofer, C. Variation in the concentration of metals in road dust size fractions between 2 µm and 2 mm: Results from three metallurgical centres in Poland. *Arc. Environ. Contam. Toxicol.* **2020**, *78*, 46–59. [[CrossRef](#)] [[PubMed](#)]
17. Patra, A.; Colville, R.; Arnold, S.; Bowen, E.; Shallcross, D.; Martin, D.; Price, C.; Tate, J.; ApSimon, H.; Robins, A. On street observation of particulate matter movement and dispersion due to traffic on an urban road. *Atmos. Environ.* **2008**, *42*, 3911–3926. [[CrossRef](#)]
18. Zhao, H.; Li, X.; Wang, X. Heavy metal contents of road-deposited sediment along the urban–rural gradient around Beijing and its potential contribution to runoff pollution. *Environ. Sci. Technol.* **2011**, *45*, 7120–7127. [[CrossRef](#)] [[PubMed](#)]
19. Khan, R.K.; Strand, M.A. Road dust and its effect on human health: A literature review. *Epidemiol. Health* **2018**, *40*, e2018013. [[CrossRef](#)]
20. Al-Shidi, H.; Sulaiman, H.; Al-Reasi, H.A.; Jamil, F.; Aslam, M. Human and ecological risk assessment of heavy metals in different particle sizes of road dust in Muscat, Oman. *Environ. Sci. Pollut. Res.* **2021**, *28*, 33980–33993. [[CrossRef](#)]
21. Vlasov, D.; Kosheleva, N.; Kasimov, N. Spatial distribution and sources of potentially toxic elements in road dust and its PM₁₀ fraction of Moscow megacity. *Sci. Total Environ.* **2021**, *761*, 142367. [[CrossRef](#)] [[PubMed](#)]
22. Shi, G.T.; Chen, Z.L.; Bi, C.J.; Wang, L.; Teng, J.Y.; Li, Y.S.; Xu, S.Y. A comparative study of health risk of potentially toxic metals in urban and suburban road dust in the most populated city of China. *Atmos. Environ.* **2011**, *45*, 764–771. [[CrossRef](#)]
23. Jiang, Y.; Ma, J.; Ruan, X.; Chen, X. Compound health risk assessment of cumulative heavy metal exposure: A case study of a village near a battery factory in Henan Province, China. *Environ. Sci. Process. Impacts* **2020**, *22*, 1408–1422. [[CrossRef](#)]

24. USEPA (US Environmental Protection Agency). Risk-based concentration table. In *Philadelphia, PA*; United States Environmental Protection Agency: Washington, DC, USA, 2000.
25. USEPA (US Environmental Protection Agency). *Guidelines for Carcinogenic Risk Assessment*; Risk Assessment Forum: Washington, DC, USA, 2005.
26. Middleton, D.R.S.; Watts, M.J.; Beriro, D.J.; Hamilton, E.M.; Leonardi, G.S.; Fletcher, T.; Close, R.M.; Polya, D.A. Arsenic in residential soil and household dust in Cornwall, south west England: Potential human exposure and the influence of historical mining. *Environ. Sci. Process. Impacts* **2017**, *19*, 517–527. [[CrossRef](#)] [[PubMed](#)]
27. Kuhns, H.; Etyemezian, V.; Green, M.; Hendricson, K.; Gown, M.; Barton, K.; Pitchford, M. Vehicle-based road dust emission measurement—Part II: Effect of precipitation, wintertime road sanding and street sweepers on inferred PM₁₀ emission potential from paved and unpaved roads. *Atmos. Environ.* **2003**, *37*, 4573–4582. [[CrossRef](#)]
28. Amato, F.; Alastuey, A.; de la Rosa, J.; Castanedo, Y.G.; de la Campa, A.S.; Pandolfi, M.; Lozano, A.; Gonzalez, J.C.; Querol, X. Trends of road dust emissions contributions on ambient air particulate levels at rural, urban and industrial sites in Southern Spain. *Atmos. Chem. Phys.* **2014**, *14*, 3533–3544. [[CrossRef](#)]
29. Chen, S.; Zhang, X.; Lin, J.; Huang, J.; Zhao, D.; Yuan, T.; Huang, K.; Luo, Y.; Jia, Z.; Zang, Z.; et al. Fugitive road dust PM_{2.5} emissions and their potential health impacts. *Environ. Sci. Technol.* **2019**, *53*, 8455–8465.
30. Witt, E.C.; Wronkiewicz, D.J.; Shi, H. Preliminary assessment of an economical fugitive road dust sampler for the collection of bulk samples for geochemical analysis. *J. Environ. Qual.* **2013**, *42*, 21–29. [[CrossRef](#)] [[PubMed](#)]
31. Amato, F.; Karanasiou, A.; Cordoba, P.; Alastuey, A.; Moreno, T.; Lucarelli, F.; Nava, S.; Calzolari, G.; Querol, X. Effects of road dust suppressants on PM levels in a Mediterranean urban area. *Environ. Sci. Technol.* **2014**, *48*, 8069–8077. [[CrossRef](#)] [[PubMed](#)]
32. Han, L.; Zhou, W.; Li, W.; Li, L. Impact of urbanization level on urban air quality: A case of fine particles (PM_{2.5}) in Chinese cities. *Environ. Pollut.* **2014**, *42*, 1–42. [[CrossRef](#)] [[PubMed](#)]
33. Sahu, S.; Beig, G.; Pakhi, N. Emissions inventory of anthropogenic PM_{2.5} and PM₁₀ in Delhi during Commonwealth Games 2010. *Atmos. Environ.* **2011**, *45*, 6180–6190. [[CrossRef](#)]
34. Pereira, G.; Teinila, K.; Custodio, D.; Santos, A.G.; Xian, H.; Hillamo, R.; Alves, C.; de Andrade, J.B.; da Rocha, G.O.; Kumar, P.; et al. Particulate pollutants in the Brazilian city of São Paulo: 1-year investigation for the chemical composition and source apportionment. *Atmos. Chem. Phys.* **2017**, *17*, 11943–11969. [[CrossRef](#)]
35. Amato, F.; Schaap, M.; Reche, C.; Querol, X. Road traffic: A major source of particulate matter in Europe. *Handb. Environ. Chem.* **2013**, *26*, 165–193.
36. MOE (Ministry of Environment). A Study on Atmospheric Emission Inventory Development, and the Estimation of Air Pollutant Emission Factors and Quantity. Available online: <https://scienceon.kisti.re.kr/srch/selectPORSrchReport.do?cn=TRKO201100002903> (accessed on 18 September 2021).
37. Souto-Oliveira, C.E.; Babinski, M.; Araujo, D.F.; Weiss, D.J.; Ruiz, I.R. Multi-isotope approach of Pb, Cu and Zn in urban aerosols and anthropogenic sources improves tracing of the atmospheric pollutant sources in megacities. *Atmos. Environ.* **2019**, *198*, 427–437. [[CrossRef](#)]
38. Thapalia, A.; Borrok, D.M.; Van Metre, P.C.; Musgrove, M.; Landa, E.R. Zn and Cu isotopes as tracers of anthropogenic contamination in a sediment core from an urban lake. *Environ. Sci. Technol.* **2010**, *44*, 1544–1550. [[CrossRef](#)]
39. Fekiacova, Z.; Cornu, S.; Pichat, S. Tracing contamination sources in soils with Cu and Zn isotopic ratios. *Sci. Total Environ.* **2015**, *517*, 96–105. [[CrossRef](#)]
40. Novak, M.; Sipkova, A.; Chrastny, V.; Stepanova, M.; Voldrichova, P.; Veselovsky, F.; Prechova, E.; Blaha, V.; Curik, J.; Farkas, J.; et al. Cu-Zn isotope constraints on the provenance of air pollution in Central Europe: Using soluble and insoluble particles in snow and rime. *Environ. Pollut.* **2016**, *218*, 1135–1146. [[CrossRef](#)]
41. Gioia, S.; Weiss, D.; Coles, B.; Arnold, T.; Babinski, M. Accurate and precise zinc isotope ratio measurements in urban aerosols. *Anal. Chem.* **2008**, *80*, 9776–9780. [[CrossRef](#)] [[PubMed](#)]
42. Xia, Y.; Gao, T.; Liu, Y.; Wang, Z.; Liu, C.; Wu, Q.; Qi, M.; Lv, Y.; Li, F. Zinc isotope revealing zinc's sources and transport processes in karst region. *Sci. Total Environ.* **2020**, *724*, 138191. [[CrossRef](#)] [[PubMed](#)]
43. Cong, Z.; Kang, S.; Luo, C.; Li, Q.; Huang, J.; Gao, S.; Li, X. Trace elements and lead isotopic composition of PM₁₀ in Lhasa, Tibet. *Atmos. Environ.* **2011**, *45*, 6210–6215. [[CrossRef](#)]
44. Resongles, E.; Dietze, V.; Green, D.C.; Harrison, R.M.; Ochoa-Gonzalez, R.; Tremper, A.H.; Weiss, D.J. Strong evidence for the continued contribution of lead deposited during the 20th century to the atmospheric environment in London of today. *Proc. Natl. Acad. Sci. USA* **2021**, *118*, e2102791118. [[CrossRef](#)]
45. Wu, P.C.; Huang, K.F. Tracing local sources and long-range transport of PM₁₀ in central Taiwan by using chemical characteristics and Pb isotope ratios. *Sci. Rep.* **2021**, *11*, 7593.
46. Souto-Oliveira, C.E.; Babinski, M.; Araújo, D.F.; Andrade, M.F. Multi-isotopic fingerprints (Pb, Zn, Cu) applied for urban aerosol source apportionment and discrimination. *Sci. Total Environ.* **2018**, *626*, 1350–1366. [[CrossRef](#)] [[PubMed](#)]
47. Schleicher, N.J.; Dong, S.; Packman, H.; Little, S.H.; Gonzalez, R.O.; Najorka, J.; Sun, Y.; Weiss, D.J. A global assessment of copper, zinc, and lead isotopes in mineral dust sources and aerosols. *Front. Earth Sci.* **2020**, *8*, 167. [[CrossRef](#)]
48. Jeong, H.; Choi, J.Y.; Lim, J.S.; Shim, W.J.; Kim, Y.O.; Ra, K. Characterization of the contribution of road deposited sediments to the contamination of the close marine environment with trace metals: Case of the port city of Busan (South Korea). *Mar. Pollut. Bull.* **2020**, *161*, 111717. [[CrossRef](#)] [[PubMed](#)]

49. Taylor, S.R. Abundance of chemical elements in the continental crust: A new table. *Geochim. Cosmochim. Acta.* **1964**, *8*, 1273–1285. [[CrossRef](#)]
50. Qingjie, G.; Jun, D.; Yunchuan, X.; Qingfei, W.; Ligiang, Y. Calculation pollution indices by heavy metals in ecological geochemistry assessment and a case study in parks of Beijing. *J. China Univ. Geo.* **2008**, *19*, 230–241. [[CrossRef](#)]
51. Hakanson, L. An ecological risk index for aquatic pollution control. A sedimentological approach. *Water Res.* **1980**, *14*, 975–1001. [[CrossRef](#)]
52. Rudnick, R.L.; Gao, S. *Composition of the Continental Crust*; Rudnick, R.L., Ed.; The Crust, Elsevier: Amsterdam, The Netherlands, 2003; pp. 1–64.
53. Xu, Z.Q.; Ni, S.; Tuo, X.G.; Zhang, C.J. Calculation of heavy metal's toxicity coefficient in the evaluation of potential ecological risk index. *Environ. Sci. Technol.* **2008**, *31*, 112–115.
54. Wang, N.; Wang, A.; Kong, L.; He, M. Calculation and application of Sb toxicity coefficient for potential ecological risk assessment. *Sci. Total Environ.* **2018**, *610–611*, 167–174. [[CrossRef](#)]
55. USEPA (US Environmental Protection Agency). *Risk Assessment Guidance for Superfund Vol. 1 Human Health Evaluation Manual, Part E, Supplemental Guidance from Dermal Risk Assessment*; Office of Emergency and Remedial Response: Washington, DC, USA, 2004.
56. USEPA (US Environmental Protection Agency). Exposure Factors Handbook (Final). Available online: <https://www.nrc.gov/docs/ML1400/ML14007A666.pdf> (accessed on 18 September 2021).
57. Adamiec, E.; Jarosz-Krzemińska, E. Human health risk assessment associated with contaminants in the finest fraction of sidewalk dust collected in proximity to trafficked roads. *Sci. Rep.* **2019**, *9*, 16364. [[CrossRef](#)]
58. Ferreira-Baptista, L.; De Miguel, E. Geochemistry and risk assessment of street dust in Luanda, Angola: A tropical urban environment. *Atmos. Environ.* **2005**, *39*, 4501–4512. [[CrossRef](#)]
59. Ma, L.; Abuduwaili, J.; Liu, W. Spatial distribution and health risk assessment of potentially toxic elements in surface soil of Boston Lake Basin, Central Asia. *Int. J. Environ. Res. Public Health* **2019**, *16*, 3741. [[CrossRef](#)] [[PubMed](#)]
60. Loganathan, P.; Vigneswaran, S.; Kandasamy, J. Road-deposited sediment pollutants: A critical review of their characteristics, source apportionment, and management. *Crit. Rev. Environ. Sci. Technol.* **2013**, *43*, 1315–1348. [[CrossRef](#)]
61. Adamiec, E.; Jarosz-Krzemińska, E.; Wieszala, R. Heavy metals from non-exhaust vehicle emissions in urban and motorway road dusts. *Environ. Monit. Assess.* **2016**, *188*, 369. [[CrossRef](#)]
62. Cai, K.; Li, C. Street dust heavy metal pollution source apportionment and sustainable management in a typical city-Shijiazhuang, China. *Int. J. Environ. Res. Public Health* **2019**, *16*, 2625. [[CrossRef](#)]
63. Baensch-Baltruschat, B.; Kocher, B.; Stock, F.; Reifferscheid, G. Tyre and road wear particles (TRWP)—A review of generation, properties, emission, human health risk, ecotoxicology, and fate in the environment. *Sci. Total Environ.* **2020**, *733*, 137823. [[CrossRef](#)] [[PubMed](#)]
64. Victoria, A.; Cobbina, S.J.; Dampare, S.B.; Duwiejua, A.B. Heavy metals concentration in road dust in the Bolgatanga Municipality, Ghana. *J. Environ. Poll. Human Health* **2014**, *2*, 74–80.
65. Zafra-Mejia, C.; Cutierrez-Malaxechebarria, A.; Hernandez-Pena, Y. Correlation between vehicular traffic and heavy metal concentrations in road sediments of Bogota, Colombia. *Rev. Fac. Med.* **2019**, *67*, 193–199. [[CrossRef](#)]
66. Padoan, E.; Rome, C.; Ajmone-Marsan, F. Bioaccessibility and size distribution of metals in road dust and roadside soils along a peri-urban transect. *Sci. Total Environ.* **2017**, *601–602*, 89–98. [[CrossRef](#)]
67. Zhao, H.; Li, X.; Wang, X.; Tian, D. Grain size distribution of road-deposited sediment and its contribution to heavy metal pollution in urban runoff in Beijing, China. *J. Hazard. Mater.* **2010**, *183*, 203–210. [[CrossRef](#)]
68. Bi, X.Y.; Liang, S.Y.; Li, X.D. Trace metals in soil, dust, and tree leaves of the urban environment, Guangzhou, China. *Chin. Sci. Bull.* **2013**, *58*, 222–230. [[CrossRef](#)]
69. Levesque, C.; Wiseman, C.L.S.; Beauchemin, S.; Rasmussen, P.E. Thoracic fraction (PM₁₀) of resuspended urban dust: Geochemistry, particle size distribution and lung bioaccessibility. *Geosciences* **2021**, *11*, 87.
70. Fujiwara, F.; Rebagliati, R.J.; Dawidowski, L.; Gomez, D.; Polla, G.; Pereyra, V.; Smichowski, P. Spatial and chemical patterns of size fractionated road dust collected in a megacity. *Atmos. Environ.* **2011**, *45*, 1497–1505. [[CrossRef](#)]
71. Daigo, L.; Matsuno, Y.; Adachi, Y. Substance flow analysis of chromium and nickel in the material flow of stainless steel in Japan. *Resour. Conserv. Recycl.* **2010**, *54*, 851–863. [[CrossRef](#)]
72. Li, R.; Shi, Y.; Wang, Z.; Wang, L.; Liu, J.; Jiang, W. Densification behavior of gas and water atomized 316L stainless steel powder during selective laser melting. *Appl. Surf. Sci.* **2010**, *356*, 4350–4356. [[CrossRef](#)]
73. Wang, X.; Wallinder, I.O.; Hedberg, Y. Bioaccessibility of nickel and cobalt released from occupationally relevant alloy and metal powders at simulated human exposure scenarios. *Ann. Work. Expo. Health* **2020**, *64*, 659–675. [[CrossRef](#)] [[PubMed](#)]
74. MGL (Ministry of Government Legislation). Korea Soil Quality Standard of Heavy Metals in Soil Environment Conservation Act (Law No. In 16613). Available online: <https://www.law.go.kr/> (accessed on 18 September 2021).
75. Jeong, H.; Choi, J.Y.; Ra, K. Characteristics of heavy metal pollution in road dust from urban areas: Comparison by land use types. *J. Environ. Anal. Health Toxicol.* **2020**, *23*, 101–111. [[CrossRef](#)]
76. Iijima, A.; Sato, K.; Yano, K.; Kato, M.; Kozawa, K.; Furuta, N. Emission factor for antimony in brake abrasion dusts as one of the major atmospheric antimony sources. *Environ. Sci. Technol.* **2008**, *42*, 2937–2942. [[CrossRef](#)]

77. Ondracek, J.; Schwarz, J.; Zdimal, V.; Andelova, L.; Vodicka, P.; Bizek, V.; Tsai, C.J.; Chen, S.C.; Smolik, J. Contribution of the road traffic to air pollution in the Prague city (busy speedway and suburban crossroads). *Atmos. Environ.* **2011**, *45*, 5090–5100. [CrossRef]
78. Chapa-Martínez, C.A.; Hinojosa-Reyes, L.; Hernández-Ramírez, A.; Ruiz-Ruiz, E.; Maya-Treviño, L.; Guzmán-Mar, J.L. An evaluation of the migration of antimony from polyethylene terephthalate (PET) plastic used for bottled drinking water. *Sci. Total Environ.* **2016**, *565*, 511–518. [CrossRef]
79. Dousova, B.; Lhotka, M.; Buzek, F.; Cejkova, B.; Jackova, I.; Bednar, V.; Hajek, P. Environmental interaction of antimony and arsenic near busy traffic nodes. *Sci. Total Environ.* **2020**, *702*, 134642. [CrossRef] [PubMed]
80. Iijima, A.; Sato, K.; Yano, K.; Tago, H.; Kato, M.; Kimura, H.; Furuta, N. Particle size and composition distribution analysis of automotive brake abrasion dust for the evaluation of antimony sources of airborne particulate matter. *Atmos. Environ.* **2007**, *41*, 4908–4919. [CrossRef]
81. Langner, M.; Kull, M.; Endlicher, W.R. Determination of PM₁₀ deposition based on antimony flux to selected urban surfaces. *Environ. Pollut.* **2011**, *159*, 2028–2034.
82. Bukowiecki, N.; Lienemann, P.; Hill, M.; Figi, R.; Richard, A.; Furger, M.; Rickers, K.; Falkenberg, G.; Zhao, Y.; Cliff, S.S.; et al. Real-world emission factors for antimony and other brake wear related trace elements: Size-segregated values for light and heavy duty vehicles. *Environ. Sci. Technol.* **2009**, *43*, 8072–8078. [CrossRef]
83. Garg, B.D.; Cadle, S.H.; Mulawa, P.A.; Groblicki, P.J. Brake wear particulate matter emissions. *Environ. Sci. Technol.* **2000**, *34*, 4463–4469. [CrossRef]
84. Jeong, H.; Lee, J.; Choi, J.Y.; Kim, K.T.; Kim, E.S.; Sun, C.; Park, J.K.; Ra, K. Study on dissolved and particulate heavy metals in stream water and stormwater runoff from Suyeong watershed in Busan special management area, Korea. *J. Korean Soc. Mar. Environ. Energy* **2019**, *22*, 203–214. [CrossRef]
85. Jeong, H.; Choi, J.Y.; Ra, K. Heavy metal pollution assessment in stream sediments from urban and different types of industrial areas in South Korea. *Soil. Sediment Contam.* **2021**, *30*, 804–818. [CrossRef]
86. Tanner, P.A.; Hoi-Ling, M.; Yu, P.K.N. Fingerprinting metals in street dust in Beijing, Shanghai and Hong Kong. *Environ. Sci. Technol.* **2008**, *42*, 7111–7117. [CrossRef] [PubMed]
87. Bukowiecki, N.; Gehrig, R.; Lienemann, P.; Hill, M.; Figi, R.; Buchmann, B.; Furger, M.; Richard, A.; Mohr, C.; Weimer, S.; et al. *PM10 Emission Factors of Abrasion Particles from Road Traffic (APART)*; Swiss Association of Road and Transportation Experts (VSS): Zurich, Switzerland, 2009.
88. Apegyei, E.; Bank, M.S.; Spengler, J.D. Distribution of heavy metals in road dust along an urban-rural gradient in Massachusetts. *Atmos. Environ.* **2011**, *45*, 2310–2323. [CrossRef]
89. Song, F.; Gao, Y. Size distributions of trace elements associated with ambient particulate matter in the vicinity of a major highway in the New Jersey-New York metropolitan area. *Atmos. Environ.* **2011**, *45*, 6714–6723. [CrossRef]
90. Sternbeck, J.; Sjodin, A.; Andreasson, K. Metal emissions from road traffic and the influence of resuspension—results from two tunnel studies. *Atmos. Environ.* **2002**, *36*, 4735–4744. [CrossRef]
91. Amato, F.; Pandolfi, M.; Moreno, T.; Furger, M.; Pey, J.; Alastuey, A.; Bukowiecki, N.; Prevot, A.S.H.; Baltensberger, U.; Querol, X. Sources and variability of inhalable road dust particles in three European cities. *Atmos. Environ.* **2011**, *45*, 6777–6787. [CrossRef]
92. Hwang, H.M.; Fiala, M.J.; Park, D.; Wade, T.L. Review of pollutants in urban road dust and stormwater runoff: Part 1. Heavy metals released from vehicles. *Int. J. Urban Sci.* **2016**, *20*, 334–360. [CrossRef]
93. Varrica, D.; Bardelli, F.; Dongarra, G.; Tamburo, E. Speciation of Sb in airborne particulate matter, vehicle brake linings, and brake pad wear residues. *Atmos. Environ.* **2013**, *64*, 18–24. [CrossRef]
94. Sjodin, A.; Ferm, M.; Björk, A.; Rahmberg, M.; Gudmundsson, A.; Swietlicki, E.; Johansson, C.; Gustafsson, M.; Blomqvist, G. *Wear Particles from Road Traffic: A Field, Laboratory and Modelling Study*; IVL Swedish Environmental Research Institute Ltd.: Göteborg, Sweden, 2010.
95. Pant, P.; Harrison, R.M. Estimation of the contribution of road traffic emissions to particulate matter concentrations from field measurements: A review. *Atmos. Environ.* **2013**, *77*, 78–97. [CrossRef]
96. Grigoratos, T.; Martini, G. Non-Exhaust Traffic Related Emissions. Brake and Tyre Wear PM. Literature Survey. Available online: <https://publications.jrc.ec.europa.eu/repository/handle/JRC89231> (accessed on 18 September 2021).
97. Panko, J.M.; Kreider, M.; Unice, K.M. Review of Tire Wear Emissions. In *A review of Tire Emission Measurement Studies: Identification of Gaps and Future Needs. Nonexhaust Emissions: An Urban Air Quality Problem for Public Health; Impact and Mitigation Measures 2018*; Elsevier Inc.: Amsterdam, The Netherlands, 2018.
98. Tonegawa, Y.; Sasaki, S. Development of tire-wear particles emission measurements for passenger vehicles. *Emiss. Contr. Sci. Technol.* **2021**, *7*, 56–62. [CrossRef]
99. Sanders, P.G.; Xu, N.; Dalka, T.M.; Maricq, M.M. Airborne brake wear debris: Size distribution, comparison, and a comparison of dynamometer and vehicle tests. *Environ. Sci. Technol.* **2003**, *37*, 4060–4069. [CrossRef] [PubMed]
100. Grigoratos, T.; Martini, G. Brake wear particle emissions: A review. *Environ. Sci. Pollut. Res.* **2015**, *22*, 2491–2504. [CrossRef]
101. Gualtieri, M.; Mantecca, P.; Cetta, F.; Camatini, M. Organic compounds in tire particle induce reactive oxygen species and heat-shock proteins in the human alveolar cell line A549. *Environ. Int.* **2008**, *34*, 437–442. [CrossRef] [PubMed]
102. Kreider, M.L.; Panko, J.M.; McAtee, B.L.; Sweet, L.I.; Finley, B.L. Physical and chemical characterization of tire-related particles: Comparison of particles generated using different methodologies. *Sci. Total Environ.* **2010**, *408*, 652–659. [CrossRef] [PubMed]

103. Dong, S.; Gonzalez, R.O.; Harrison, R.M.; Green, D.; North, R.; Fowler, F.; Weiss, D. Isotopic signatures suggest important contributions from recycled gasoline, road dust and non-exhaust traffic sources for copper, zinc and lead in PM₁₀ in London, United Kingdom. *Atmos. Environ.* **2017**, *165*, 88–98. [[CrossRef](#)]
104. Sugden, C.L.; Farmer, J.G.; MacKenzie, A.B. Isotopic ratios of lead in contemporary environmental material from Scotland. *Environ. Geochem. Health* **1993**, *15*, 59–65. [[CrossRef](#)]
105. LeGalley, E.; Widom, E.; Krekeler, M.P.S.; Kuentz, D.C. Chemical and lead isotope constraints on sources of metal pollution in street sediment and lichens in southwest Ohio. *Appl. Geochem.* **2013**, *32*, 195–203. [[CrossRef](#)]
106. O’Shea, M.J.; Krekeler, M.P.S.; Vann, D.R.; Gieré, R. Investigation of Pb-contaminated soil and road dust in a polluted area of Philadelphia. *Environ. Monit. Assess.* **2021**, *193*, 440. [[CrossRef](#)] [[PubMed](#)]
107. Hunt, A. Relative bioaccessibility of Pb-based paint in soil. *Environ. Geochem. Health* **2016**, *38*, 1037–1050. [[CrossRef](#)]
108. O’Connor, D.; Hou, D.; Ye, J.; Zhang, Y.; Ok, Y.S.; Song, Y.; Coulon, F.; Peng, T.; Tian, L. Lead-based paint remains a major public health concern: A critical review of global production, trade, use, exposure, health risk, and implications. *Environ. Int.* **2018**, *121*, 85–101. [[PubMed](#)]
109. Jeong, H.; Ra, K. Multi-isotope signatures (Cu, Zn, Pb) of different particle sizes in road-deposited sediments: A case study from industrial area. *J. Anal. Sci. Technol.* **2021**, *12*, 39. [[CrossRef](#)]
110. Han, Y.; Wang, Z.; Zhou, J.; Che, H.; Tian, M.; Wang, H.; Shi, G.; Yang, F.; Zhang, S.; Chen, Y. PM_{2.5}-bound heavy metals in Southwestern China: Characterization, sources, and health risks. *Atmosphere* **2021**, *12*, 929. [[CrossRef](#)]
111. Kim, M.S.; Kim, J.Y.; Park, J.; Yeon, S.H.; Shin, S.; Choi, J. Assessment of pollution sources and contribution in urban dust using metal concentrations and multi-isotope ratios (¹³C, ²⁰⁷/²⁰⁶Pb) in a complex industrial port area, Korea. *Atmosphere* **2021**, *12*, 840. [[CrossRef](#)]
112. Souto-Oliveira, C.E.; Kamigauti, L.Y.; Andrade, M.F.; Babinski, M. Improving source apportionment of urban aerosols using multi-isotopic fingerprints (MIF) and positive matrix factorization (PMF): Cross-validation and new insights. *Front. Environ. Sci.* **2021**, *9*, 623915. [[CrossRef](#)]